appended fluorophore. A further increase in pH does not influence the position of the side chain, but simply increases the quenching efficiency. Most of the previously reported fluorescence switches typically exhibit two states: on or off.[10, 11] Systems displaying multistage emission are more rare and include 2-naphthol[12] and a tin(IV) complex of a functionalized porphyrin.[13] Ligand **2** is a novel high/low/off fluorescence switch whose control has a mechanical nature.

Experimental Section

3: 2-Bromoethylamine was allowed to react with a stoichiometric amount of 9-anthracenecaraldehyde in CH_2Cl_2. The reaction mixture was dried over Na_2SO_4, filtered, and evaporated to dryness. The residue was recrystallized from *n*-hexane/diethyl ether (1/1); yield 45%. Correct C,H,N analysis.

2: Cyclam (0.48 g, 2.4 mmol) was disolved in hot toluene, and **3** (0.14 g, 0.45 mmol) added as a solid. The resulting solution was heated at reflux for 3 h and then cooled to room temperature. The ammonium salts of excess cyclam were removed by filtration, and the clear solution extracted with 0.1M NaOH to separate the remaining cyclam. The dried organic layer was filtered and evaporated to dryness. The resulting yellow oily substance was dissolved in EtOH (20 mL) and reduced with excess $NaBH_4$. Compound **2** was obtained as a pale yellow oil; yield (based on **3**) 70%. MS (ESI): 434 $[M+H^+]$. The NMR spectra were consistent with the proposed structure.

$[Ni^{II}(\mathbf{2})](ClO_4)_2 \cdot H_2O$: **2** (150 mg, 0.35 mmol) was dissolved in EtOH (30 mL), and a stoichiometric amount of an aqueous solution of 0.55M $Ni(ClO_4)_2$ added. The obtained mixture was heated at reflux for 2 h and then evaporated to dryness. The residue was recrystallized from water. $[Ni^{II}(\mathbf{2})](ClO_4)_2 \cdot H_2O$ was obtained as a pale brown solid; yield 63%. Correct C,H,N analysis; MS (ESI): 590 $[M - ClO_4]$.

Received: June 11, 1997
Revised version: November 7, 1997 [Z10535IE]
German version: *Angew. Chem.* **1998**, *110*, 838–841

Keywords: fluorescence · electron transfer · macrocycles · molecular devices · nickel

[1] R. A. Bissell, E. Córdova, A. E. Kaifer, J. F. Stoddart, *Nature* **1994**, *369*, 133.
[2] A. Livoreil, C. O. Dietrich-Buchecker, J. P. Sauvage *J. Am. Chem. Soc.* **1994**, *116*, 9399.
[3] D. J. Cárdenas, A. Livoreil, J. P. Sauvage, *J. Am. Chem. Soc.* **1996**, *118*, 11980.
[4] R. Ballardini, V. Balzani, M. T. Gandolfi, L. Prodi, M. Venturi, D. Philp, H. G. Ricketts, J. F. Stoddart, *Angew. Chem.* **1993**, *105*, 1363; *Angew. Chem. Int. Ed. Engl.* **1993**, *32*, 1301.
[5] T. A. Kaden, *Top. Curr. Chem.* **1984**, *121*, 157.
[6] P. Pallavicini, A. Perotti, B. Seghi, L. Fabbrizzi, *J. Am. Chem. Soc.* **1987**, *109*, 5139.
[7] The quantum yield for $[Ni^{II}(B\text{-}LH^+\text{-}An)]^{3+}$ is 0.083 in EtOH (0.27 for plain anthracene).
[8] The isolated component $[Ni^{II}(cyclam)]^{2+}$ quenches the emission of the reference compound $AnCH_2NH_2^+C_3H_7$ in aqueous MeCN by a bimolecular process. Reduction of I_F to 10% requires the addition of 4500 equivalents of $[Ni^{II}(cyclam)]^{2+}$. This emphasizes the "chelate effect" exerted by the aliphatic linker, which favors the intramolecular metal–fluorophore collisions in $[Ni^{II}(B\text{-}LH^+\text{-}An)]^{3+}$.
[9] One of the referees made the hypothesis that at pH 10 or above, a species of the composition $[Ni^{II}(B\text{-}L\text{-}An)(OH)Ni^{II}(B\text{-}L\text{-}An)]^{3+}$ could form: In this dinuclear species each cyclam subunit coordinates to its metal in a *cis* fashion, and the hydroxo group bridges the two Ni^{II} centers. Although hydroxo-bridged complexes are often observed in transition metal complexes in basic solution, this possibility can be ruled out in the present case: Complete quenching of fluorescence requires the addition of 2 equiv of OH^-, whereas 1.5 equiv are needed for the formation of the dinuclear species $[Ni^{II}(B\text{-}L\text{-}An)(OH)Ni^{II}(B\text{-}L\text{-}An)]^{3+}$. Furthermore, $[Ni^{II}(B\text{-}L\text{-}An)(OH)Ni^{II}(B\text{-}L\text{-}An)]^{3+}$, when replacing $[Ni^{II}(B\text{-}L\text{-}An)(OH)]^+$, did not fit well with the potentiometric titration data.
[10] A. P. de Silva, H. Q. N. Gunaratne, T. Gunnlaugsson, A. J. M. Huxley, C. P. McCoy, J. T. Rademacher, T. E. Rice, *Chem. Rev.* **1997**, 97, 1515.
[11] L. Fabbrizzi , A. Poggi, *Chem. Soc. Rev.* **1995**, 197.
[12] W. Klöpffer, *Adv. Photochem.* **1977**, *10*, 312.
[13] R. Grigg, W. D. J. A. Norbert, *J. Chem. Soc. Chem. Commun.* **1992**, 1298.

SIAM, a Novel NMR Experiment for the Determination of Homonuclear Coupling Constants**

Thomas Prasch, Peter Gröschke, and Steffen J. Glaser*

The most important NMR parameters for the determination of molecular conformations in solution are cross-relaxation rates and coupling constants.[1] With the help of empirical Karplus relations, vicinal coupling constants (^3J) yield information about dihedral angles. For example, in peptides and proteins the $^3J(H^N,H^\alpha)$ coupling is related to the backbone angle ϕ.[2] However, the quantitative determination of coupling constants is difficult if the line width is not significantly smaller than the coupling constants of interest (Figure 1). In the case of in-phase doublets (e.g. in NOESY[3]

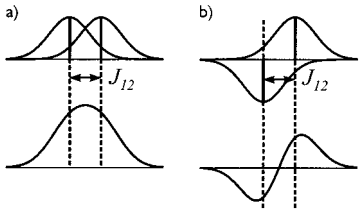

Figure 1. The apparent splittings of in-phase (a) and antiphase (b) doublets deviate markedly from the actual coupling constant J_{12} if the line width is not much smaller than J_{12}.[6] The individual doublet components are shown at the top and their superposition is shown at bottom. In this case the superimposed in-phase signal does not show any resolved splitting (a), whereas the apparent splitting of the superimposed antiphase signal is significantly larger than the coupling constant J_{12} (b).

[*] Priv.-Doz. Dr. S. J. Glaser, Dipl.-Chem. T. Prasch, Dipl.-Chem. P. Gröschke
Institut für Organische Chemie der Universität
Marie-Curie-Strasse 11, D-60439 Frankfurt (Germany)
Fax: (+49) 69-7982-9128
E-mail: sg@org.chemie.uni-frankfurt.de

[**] This work was supported by the Deutsche Forschungsgesellschaft (Gl 203/2-1 and Gl 203/1-5) and by the Fonds der Chemischen Industrie. T. P. thanks the Fonds der Chemischen Industrie for a doctoral fellowship and the Graduiertenkolleg (Gk oIII Eg-52/3-3) for support. All experiments were performed at the Large Scale Facility "Center for Biomolecular NMR at the University of Frankfurt"-(ERBFMGECT950034).

  1433-7851/98/3706-0802 $ 17.50+.50/0

or TOCSY spectra[4]) the finite line width results in a reduced separation of the maxima of the two doublet lines (Figure 1a). This is in contrast to the case of antiphase doublets (e.g. in DQF-COSY spectra[5]), where the finite line width leads to an increased separation of the doublet maxima and hence to an apparent splitting that is larger than the actual coupling constant (Figure 1b).[6] However, the precise determination of coupling constants is possible irrespective of the experimental line form if both in-phase and antiphase multiplets are available.[7, 8]

Here we present a new experimental approach for the simultaneous acquisition of in-phase and antiphase multiplets that provides spectra with a minimum of overlap and markedly enhanced sensitivity compared to conventional methods. The experiment is based on the fact that several coherence transfer processes occur simultaneously during the mixing period τ of TOCSY experiments. For example, in a spin system consisting of two spins 1/2, polarization of the first spin (I_{1z}) is transformed not only into polarization of the second spin (I_{2z}), but also into zero-quantum coherence ($ZQ_y = I_{1y}I_{2x} - I_{1x}I_{2y}$) between the two spins [Eq. (1)].[4]

$$I_{1z} \rightarrow I_{1z}\cos^2(\pi J_{12}\tau) + I_{2z}\sin^2(\pi J_{12}\tau) - ZQ_y\sin(2\pi J_{12}\tau) \quad (1)$$

In conventional TOCSY experiments only the polarization transfer $I_{1z} \rightarrow I_{2z}$ is exploited, resulting in cross peaks with in-phase splitting in ω_1 and ω_2 (Figure 2a). The second transfer

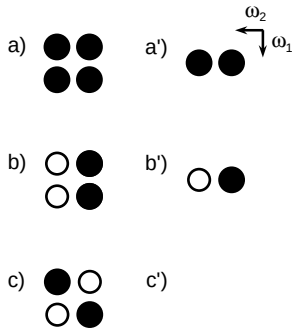

Figure 2. Schematic representation of characteristic multiplets in 2D NMR spectra: a) in-phase splitting in ω_1 and ω_2 (e.g. NOESY, ROESY, TOCSY, and ZQF-SIAM), b) in-phase splitting in ω_1 and antiphase splitting in ω_2 (DQF-SIAM), c) antiphase splitting in ω_1 and ω_2 (e.g. DQF-COSY). Positive signals are white, negative signals are black. a′)–c′) show the corresponding multiplets when ω_1 decoupling is used. In the first two cases this leads to a signal enhancement and to an improved resolution, whereas in the third case the signals completely cancel.

($I_{1z} \rightarrow ZQ_y$), which results in an in-phase splitting in ω_1 and an antiphase splitting in ω_2 (Figure 2b), was so far either ignored or suppressed.[4] The separation of polarization I_{2z} and zero-quantum coherence ZQ_y poses a problem because both terms have the same coherence order $p = 0$.[1] However, if the two mutually coupled spins have well-resolved chemical shifts, selective pulses can be used to convert the zero-quantum coherence ZQ_y selectively into double-quantum coherence ($DQ_y = I_{1y}I_{2x} + I_{1x}I_{2y}$) with coherence order $p = \pm 2$. The two terms I_{2z} and DQ_y can be conveniently selected with the help of a zero-quantum filter (ZQF) and a double-quantum filter (DQF), respectively (Figure 3a). It is even possible to realize

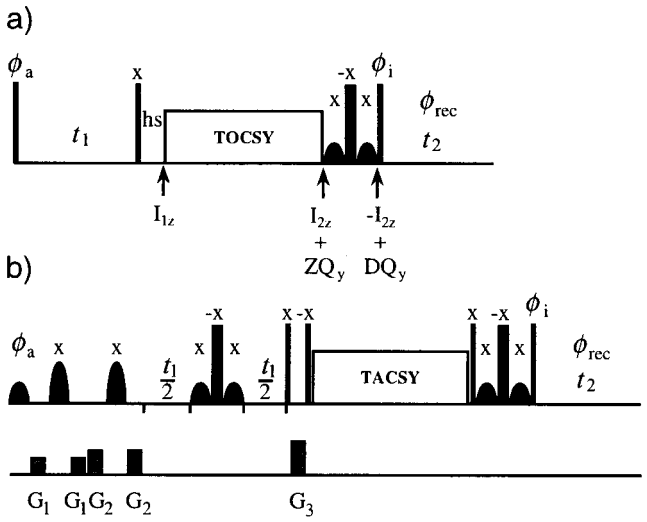

Figure 3. a) Schematic pulse sequence of a SIAM experiment (narrow vertical lines: 90° pulses; broad vertical lines: 180° pulses; bell-shaped symbols: selective 90° pulses acting only on spin I_1; hs: homospoil gradient; phase cycles of ϕ_a, ϕ_i, and ϕ_{rec}: see Experimental Section). For a two-spin system, the characteristic operators created during the sequence are indicated. b) Optimized SIAM experiment for the determination of $^3J(H^N,H^\alpha)$ couplings in peptides and proteins (see Experimental Section).

both filters by processing a single experimental data set in two different ways (see Experimental Section). Since this allows the *s*imultaneous acquisition of *i*n-phase and *a*ntiphase *m*ultiplets, we refer to the new method as the SIAM experiment. Because the cross peaks of both ZQF-SIAM and DQF-SIAM spectra have an in-phase splitting in ω_1, it is possible to further increase the resolution and the sensitivity by ω_1 decoupling[9](Figure 2a′, b′). This is not possible in a conventional DQF-COSY experiment with antiphase splittings in ω_1 and ω_2 (Figure 2c, c′). Figure 3b shows an optimized SIAM experiment with ω_1 decoupling and band-selective excitation for the quantitative determination of $^3J(H^N,H^\alpha)$ couplings in peptides and proteins. In addition, a band-selective TACSY mixing sequence (*ta*ilored *c*orrelation *s*pectroscopy)[10] is used which provides more efficient coherence transfer than a nonselective TOCSY sequence (*to*tal *c*orrelation *s*pectroscopy) (see Experimental Section).

Figures 4a and b show a section of the fingerprint region of the protein BPTI with H^N,H^α cross peaks; the ZQF-SIAM and DQF-SIAM spectra were obtained from the same experimental SIAM data set. For comparison, Figure 4c shows the corresponding region of a conventional DQF-COSY spectrum (same total measurement time). The resolution of the DQF-SIAM spectrum (Figure 4b) is markedly better than that of the DQF-COSY spectrum because of ω_1 decoupling. Furthermore, the intensity of the antiphase signals is significantly larger in the DQF-SIAM experiment. For example, the cross sections of the DQF-SIAM cross peaks of Ala 25, Ala 58, and Ile 18 are up to a factor of four more intense than those of the corresponding DQF-COSY cross peaks (see Figure 5). The fact that a ZQF-SIAM spectrum with in-phase splitting and a DQF-SIAM spectrum with antiphase splitting can be obtained from the same data set not only saves measurement time, but also guarantees that the in-phase and antiphase multiplets have identical center frequencies. This is not

  1433-7851/98/3706-0803 $ 17.50+.50/0

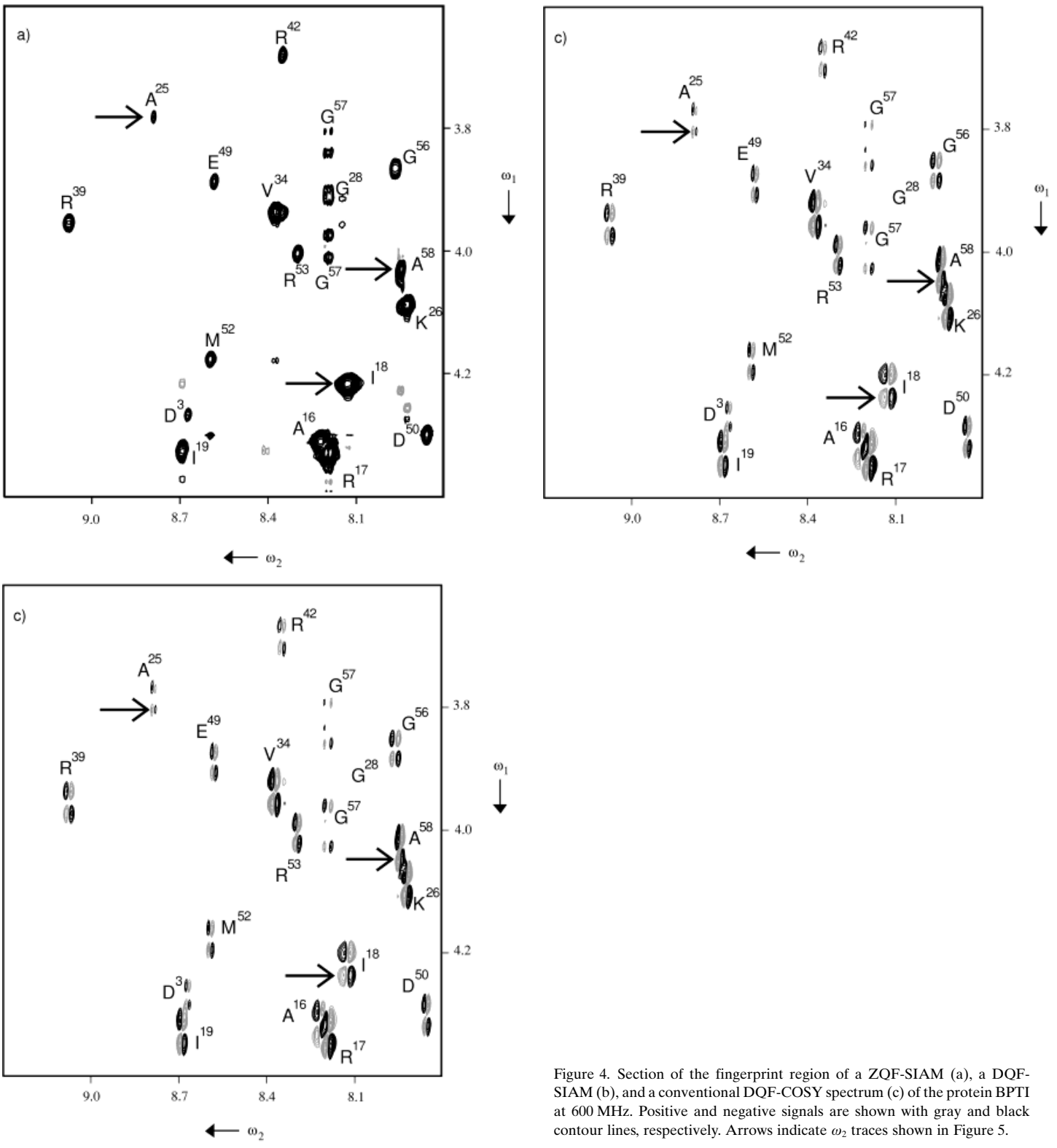

Figure 4. Section of the fingerprint region of a ZQF-SIAM (a), a DQF-SIAM (b), and a conventional DQF-COSY spectrum (c) of the protein BPTI at 600 MHz. Positive and negative signals are shown with gray and black contour lines, respectively. Arrows indicate ω_2 traces shown in Figure 5.

warranted if two different experiments (e.g. DQF-COSY and TOCSY) are acquired because of nonidentical sample heating. Hence, the novel SIAM experiment is almost ideally suited for the determination of $^3J(H^N,H^\alpha)$ coupling constants in peptides and proteins. Based on the traces of the ZQF-SIAM and DQF-SIAM cross peaks shown in Figure 5, $^3J(H^N,H^\alpha)$ coupling constants of (3.6 ± 0.25) Hz for Ala 25, (6.1 ± 0.25) Hz for Ala 58, and (9.7 ± 0.25) Hz for Ile 18 were determined by using the Keeler–Titman extraction procedure.[8] These coupling constants differ significantly from the apparent in-phase splittings of 0, 6.3, and 6.5 Hz, respectively.

  1433-7851/98/3706-0804 $ 17.50+.50/0

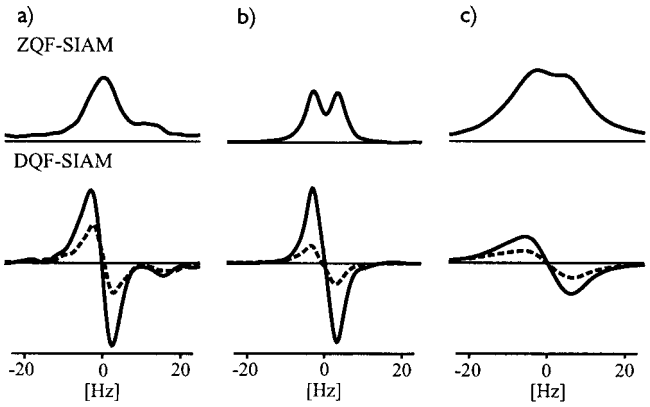

Figure 5. ω_2 traces of the (H^N,H^α) cross peaks of a) Ala 25, b) Ala 58, and c) Ile 18 (see arrows in Figure 4) with representative $^3J(H^N,H^\alpha)$ coupling constants and line widths. The top panels show the in-phase signals of the ZQF-SIAM spectrum and the bottom panels show the antiphase signals of the DQF-SIAM spectrum (solid lines). The dashed lines represent the antiphase signals of the conventional DQF-COSY spectrum for comparison.

The SIAM method is not restricted to the determination of $^3J(H^N,H^\alpha)$ couplings nor to applications to peptides and proteins. A necessary condition is that the two mutually coupled spins of interest (here H^N and H^α) have different chemical shifts. Furthermore it must be ensured that in large spin systems the pure in-phase and antiphase multiplets are not contaminated by other signals. A sufficient (but not necessary) condition for this is that the detected spin (here H^N) has no further coupling partners. Hence, the SIAM method complements the powerful E.COSY technique,[11] for which a third common coupling partner is mandatory.

Experimental Section

The SIAM technique is based on the conversion of zero-quantum coherence ZQ_y to double-quantum coherence DQ_y, which requires a band-selective inversion pulse with a simultaneous suppression of chemical shift evolution. This can be implemented by a composite pulse element consisting of a hard (nonselective) 180°_{-x} pulse sandwiched between two band-selective 90°_x pulses (see Figure 3). A ZQF- and a DQF-SIAM spectrum can be obtained from the same experimental data set if for each t_1 increment two free induction decays FID1(t_1,t_2) and FID2(t_1,t_2) with different phase cycles are acquired and stored separately. The phase cycle ϕ_i of the last 90° pulse (Figure 3) and the phase ϕ_{rec} of the receiver are ϕ_i = x, − x and ϕ_{rec} = x, − x for FID1(t_1,t_2), whereas for FID2(t_1,t_2) ϕ_i = y, − y and ϕ_{rec} = y, − y. Addition and subtraction of FID1(t_1,t_2) and FID2(t_1,t_2) yields, after a two-dimensional Fourier transformation, a ZQF- and a DQF-SIAM spectrum, respectively. Only an additional 90° phase correction in ω_2 is required for the DQF-SIAM spectrum.

The spectra shown in Figures 4 and 5 were acquired with the SIAM experiment shown in Figure 3b, which was optimized for the determination of $^3J(H^N,H^\alpha)$ couplings in peptides and proteins. The RF irradiation frequency was positioned at 6.2 ppm. The water signal was presaturated by CW irradiation for a duration of 2 s (not shown in Figure 3b). For band-selective excitation we used a H^α-selective 90° pulse (Q5)[12] with a duration of 3.731 ms and an offset of − 1.072 kHz in combination with two H^α-selective 180° pulses (Q3)[12] with a duration of 3 ms and an offset of − 1.072 kHz. (Offset frequency, amplitude, and duration of the band-selective pulses are matched for experiments at 600 MHz but can be scaled for applications at other spectrometer frequencies.) The two H^α-selective 180° pulses were bracketed by different B_0 gradients (G_1 = 15 G cm^{-1}, G_2 = 25 G cm^{-1}) with a duration of 1 ms each.[13] This made it possible to reduce the spectral width in ω_1 to 1 kHz and the number of t_1 increments to 200 (spectral width in ω_2: 4.194 kHz, 2048 complex data points in t_2). The phase ϕ_a was incremented by using the TPPI scheme.[14] A composite pulse consisting of two H^α-selective 90°_x pulses (Q5)and a nonselective 180°_{-x} pulse was used both for ω_1 decoupling in the center of t_1 and for the conversion of zero-quantum coherence ZQ_y to double-quantum coherence DQ_y at the end of the sequence. Prior to the mixing step, x magnetization was selected by two 90°_y pulses and a B_0 gradient (G_3 = 35 G cm^{-1}). The band-selective HNHA-TACSY sequence CABBY-1[10] was used in the mixing period. The radio frequency amplitude of CABBY-1 was 4.4 kHz, corresponding to a bandwidth of about 3.4 kHz, which allows efficient polarization and coherence transfer between H^α and H^N (in the range between 3.4 and 9.0 ppm). The mixing time used was 43 ms (according to relation (1) the optimal mixing time for the creation of zero-quantum coherence ZQ_y between H^N and H^α is given by $\tau = 1/(4J_{12})$ with $J_{12} = {}^3J(H^N,H^\alpha)$). For the clean conversion of ZQ_y to DQ_y it is important that the H^N spins can be inverted without affecting the H^α spins. This is usually possible because the H^N and H^α resonances are well separated. Overlap between H^α and H^β resonances (e.g. of Ser or Thr) does not pose a problem. Although this leads to a loss of sensitivity (due to incomplete ω_1 decoupling of the $^3J(H^\alpha,H^\beta)$ couplings and nonselective TOCSY transfer), the additional coherence terms (involving more than two spins) do not lead to any detectable signals if not all participating spins are coupled to the detected spin (H^N). As $^4J(H^N,H^\beta)$ couplings can be neglected, the H^α,H^N cross peaks in ZQF-SIAM and DQF-SIAM spectra show even in the presence of overlapping H^α and H^β resonances purely absorptive in-phase and antiphase splittings with respect to the desired $^3J(H^N,H^\alpha)$ coupling. (Only in the case of Gly, where H^N is coupled to H^α and $H^{\alpha'}$, can the H^α,H^N cross peaks of the ZQF-SIAM spectrum can contain in addition to the desired absorptive in-phase signals also dispersive signals in double antiphase with respect to H^α and $H^{\alpha'}$).

A SIAM experiment and a DQF-COSY experiment were acquired for the protein BPTI at a temperature of 310 K using the same band-selective excitation and the same total measurement time of 9.5 h with a total of 64 scans per t_1 increment (32 scans for FID1(t_1,t_2) and 32 scans for FID2(t_1,t_2) in the SIAM experiment). Except for the addition and subtraction of FID1(t_1,t_2) and FID2(t_1,t_2) for the ZQF-SIAM and DQF-SIAM spectrum, respectively, and an additional 90° phase correction (0th order) in ω_2 for the DQF-SIAM spectrum (as described above), the 2D spectra shown in Figure 4 were processed and scaled identically (no apodization in ω_2, skewed sinebell with a phase of 90° and a skew parameter of 0.8 in ω_1, polynomial baseline correction in ω_1 und ω_2). In order to increase the digital resolution of the traces shown in Figure 5, the traces were inversely Fourier transformed and the first 1024 points of the resulting interferograms were extended to 16384 points by using linear prediction with 110 poles. After a final Fourier transformation, the digital resolution of the traces was 0.25 Hz per point.

Received: July 30, 1997 [Z10752IE]
German version: *Angew. Chem.* **1998**, *110*, 817 – 821

Keywords: NMR spectroscopy · peptides · proteins · structure elucidation

[1] a) K. Wüthrich, *NMR of Proteins and Nucleic Acids*, Wiley, New York, **1986**; b) H. Kessler, M. Gehrke, C. Griesinger, *Angew. Chem.* **1988**, *100*, 507 – 554; *Angew. Chem. Int. Ed. Engl.* **1988**, *27*, 490 – 536; c) *Two-Dimensional NMR Spectroscopy* (Eds.: W. R. Croasmun, R. M. K. Carlson), VCH Publishers, New York, **1994**.

[2] A. Pardi, M. Billeter, K. Wüthrich, *J. Mol. Biol.* **1984**, *180*, 741 – 751.

[3] a) J. Jeener, B. H. Meier, P. Bachmann, R. R. Ernst, *J. Chem. Phys.* **1979**, *71*, 4546 – 4553; b) S. Macura, Y. Huang, D. Suter, R. R. Ernst, *J. Magn. Reson.* **1981**, *43*, 259 – 281.

[4] a) L. Braunschweiler, R. R. Ernst, *J. Magn. Reson.* **1983**, *53*, 521 – 528; b) A. Bax, D. G. Davis, *ibid.* **1985**, *65*, 355 – 360; c) S. J. Glaser, J. J. Quant in *Advances in Magnetic and Optical Resonance, Vol. 19* (Ed.: W. Warren), Academic Press, San Diego, **1996**, pp. 59 – 252.

[5] a) U. Piantini, O. W. Sørensen, R. R. Ernst, *J. Am. Chem. Soc.* **1982**, *104*, 6800 – 6801; b) M. Rance, O. W. Sørensen, G. Bodenhausen, G. Wagner, R. R. Ernst, K. Wüthrich, *Biochem. Biophys. Res. Commun.* **1983**, 117, 479 – 485.

  1433-7851/98/3706-0805 $ 17.50+.50/0

[6] a) D. Neuhaus, G. Wagner, M. Vasak, J. H. R. Kägi, K. Wüthrich, *Eur. J. Biochem.* **1985**, *151*, 257–273; b) M. Eberstadt, G. Gemmecker, D. F. Mierke, H. Kessler, *Angew. Chem.* **1995**, *107*, 1813–1838; *Angew. Chem. Int. Ed. Engl.* **1995**, *34*, 1671–1695.
[7] a) H. Oschkinat, R. Freeman, *J. Magn. Reson.* **1984**, *60*, 164–169; b) H. Kessler, S. Seip in ref.[1c], pp. 619–654.
[8] a) J. Titman, J. Keeler, *J. Magn. Reson.* **1990**, *89*, 640–646; b) P. Huber, C. Zwahlen, S. J. F. Vincent, G. Bodenhausen, *J. Magn. Reson. A* **1993**, 103, 118–121.
[9] R. Brüschweiler, C. Griesinger, O. W. Sørensen, R. R. Ernst, *J. Magn. Reson.* **1988**, *78*, 178–185.
[10] J. Quant, T. Prasch, S. Ihringer, S. J. Glaser, *J. Magn. Reson. B* **1995**, *106*, 116–121.
[11] a) C. Griesinger, O. W. Sørensen, R. R. Ernst, *J. Am. Chem. Soc.* **1985**, *107*, 6394–6396; b) C. Griesinger, O. W. Sørensen, R. R. Ernst, *J. Chem. Phys.* **1986**, *85*, 6837–6852; c) C. Griesinger, O. W. Sørensen, R. R. Ernst, *J. Magn. Reson.* **1987**, *75*, 474–492.
[12] L. Emsley, G. Bodenhausen, *J. Magn. Reson.* **1992**, *97*, 135–148.
[13] T. L. Hwang, A. J. Shaka, *J. Magn. Reson. A* **1995**, *112*, 275–279.
[14] D. Marion, K. Wüthrich, *Biochem. Biophys. Res. Commun.* **1983**, *113*, 967–974.

Catalytic Hydrogenolysis at Low Temperature and Pressure of Polyethylene and Polypropylene to Diesels or Lower Alkanes by a Zirconium Hydride Supported on Silica-Alumina: A Step Toward Polyolefin Degradation by the Microscopic Reverse of Ziegler–Natta Polymerization

Véronique Dufaud* and Jean-Marie Basset*

Transition metal catalyzed polymerization of ethylene and propylene was discovered in the 1950s by Ziegler and Natta.[1] Since then, there have been many applications and a large production of these polymers. However, at the end of this century, the presence of such polyolefins in our daily life has reached such a level that its environmental consequences can no longer be underestimated. The solutions to overcome this environmental challenge with catalytic methods at low temperature and pressure are not known at the moment.[2] The scientific reasons for this deficit may be divided in two categories: the chemical inertness of polyolefins and the thermodynamic limitations to achieving the reverse of the Ziegler–Natta polymerization.

Although they are formed from olefins, polyolefins such as polyethylene or polypropylene are not "olefinic" materials since they become "paraffinic" upon polymerization. These long-chain paraffinic materials are extremely inert, and there is no simple way to transform them selectively, especially at moderate temperature, into valuable products.

[*] Dr. V. Dufaud, Dr. J.-M. Basset
Laboratoire de Chimie Organométallique de Surface
UMR 9986, CNRS-CPE Lyon
43 boulevard du 11 Novembre 1918, 69616 Villeurbanne Cédex (France)
Fax: (+33) 47243-1793
E-Mail: basset@coms1.cpe

It would be very fascinating to transform polyolefins into olefinic oligomers or monomers, which is theoretically possible from a mechanistic point of view according to the principle of microreversibility. The insertion of an olefin into a metal–alkyl bond, the key step in the Ziegler–Natta polymerization,[3] can be considered as the microscopic reverse of the β-alkyl transfer [Eq. (a); the polymer chain is

(a)

represented by Ⓟ].[4] However, since such transformations are thermodynamically impossible at moderate temperature, it is necessary to find solutions to overcome this limitation.

We report here that it is possible to polymerize ethylene or propylene to the corresponding polyolefins with a zirconium hydride supported on silica-alumina.[5] We also demonstrate that under hydrogen the same catalyst that can polymerize ethylene or propylene is able to cleave statistically all the C–C bonds of polyethylene or polypropylene to a range of short-chain saturated oligomers, diesels, or eventually methane, ethane, and lower alkanes.

We recently disclosed a new catalyst that is able to carry out the catalytic cleavage of the C–C bonds in several simple alkanes under hydrogen. The catalyst is a well-defined silica-supported zirconium monohydride ($\equiv SiO)_3ZrH$ (**1**)[6–8] that is obtained by surface organometallic chemical reactions.[9] For example, **1**, which is very electrophilic,[10] is able to cleave the C–C bonds of propane, butanes, and pentanes (but not ethane) under a moderate hydrogen pressure (<1 atm) and at mild temperatures (typically 25–150 °C).[11, 12] Considering that polyolefins are simply long-chain hydrocarbons, the catalytic cleavage of the C–C bonds in these higher alkanes might be possible with our electrophilic silica-supported zirconium hydride or some more strongly electrophilic supported zirconium hydride.

To render the supported zirconium hydride even more electrophilic than on silica, we treated tetraneopentylzirconium with the surface silanol groups of a silica-alumina that was partially dehydroxylated at 500 °C (silica-alumina$_{500}$). The reaction led to the formation of a surface species which can be formulated as $(\equiv SiO)ZrNp_3$ (**2**). Treatment of **2** with hydrogen at 150 °C provided the formation of a zirconium hydride supported on silica-alumina with the concommitant generation of silicon dihydride and aluminium hydride. Based on what is known for the structure of **1** on pure silica, we propose two structures for the zirconium hydride supported on silica-alumina (Scheme 1): One can be formulated as $(\equiv SiO)_3ZrH$ (**3a**), in which the zirconium hydride is a monohydride grafted to silica-alumina through three covalent bonds. This was already demonstrated for pure silica by several techniques including EXAFS.[8] The second structure **3b** is very similar. However, aluminium hydride groups could be in close proximity to the zirconium center, and the zirconium atom would be even more electrophilic than on pure silica.

When **3** was exposed to an ethylene pressure of 200 torr at room temperature, the IR spectrum of the solid showed the

  1433-7851/98/3706-0806 $ 17.50+.50/0